The American Journal of Pathology, Vol. 185, No. 2, February 2015

The American Journal of
PATHOLOGY
ajp.amjpathol.org

NEUROBIOLOGY

Astrocytic Dynamin-Like Protein 1 Regulates Neuronal Protection against Excitotoxicity in Parkinson Disease

Jake G. Hoekstra,* Travis J. Cook,† Tessandra Stewart,* Hayley Mattison,* Max T. Dreisbach,* Zachary S. Hoffer,* and Jing Zhang*

From the Department of Pathology, University of Washington, Seattle; and the Department of Environmental and Occupational Health Sciences,† University of Washington School of Public Health, Seattle, Washington*

Accepted for publication October 7, 2014.

Address correspondence to Jing Zhang, M.D., Ph.D., Department of Pathology, University of Washington, School of Medicine, Box 359635, 325 9th Ave, Seattle, WA 98104. E-mail: zhangj@uw.edu.

Mitochondrial dynamics has recently become an area of piqued interest in neurodegenerative disorders, including Parkinson disease (PD); however, the contribution of astrocytes to these disorders remains unclear. Here, we show that the level of dynamin-like protein 1 (Dlp1; official name *DNM1L*), which promotes mitochondrial fission, is lower in astrocytes from the brains of PD patients, and that decreased astrocytic Dlp1 likely represents a relatively early event in PD pathogenesis. In support of this conclusion, we show that Dlp1 knockdown dramatically affects mitochondrial morphological characteristics and localization in astrocytes, impairs the ability of astrocytes to adequately protect neurons from the excitotoxic effects of glutamate, and increases intracellular Ca^{2+} in response to extracellular glutamate, resulting from compromised intracellular Ca^{2+} buffering. Taken together, our results suggest that astrocytic mitochondrial Dlp1 is a key protein in mitochondrial dynamics and decreased Dlp1 may interfere with neuron survival in PD by disrupting Ca^{2+}-coupled glutamate uptake. *(Am J Pathol 2015, 185: 536–549; http://dx.doi.org/10.1016/j.ajpath.2014.10.022)*

Parkinson disease (PD) is a neurodegenerative disorder clinically characterized by both motor and nonmotor symptoms.[1–3] The loss of dopaminergic (DAergic) neurons in the substantia nigra pars compacta (SNpc) is the primary cause of the motor deficits,[4] whereas nonmotor symptoms are the result of dysfunction in multiple brain regions.[2,3] Until recently, most investigations have focused on the neuronal pathogenesis. However, accumulating evidence shows that astrocytes, which have multiple neuroprotective roles,[5,6] contribute to neuronal loss in PD.[7]

Decreased respiratory chain activity[8] and increased oxidative damage in the SNpc[9,10] contribute to neuronal demise in PD. Among proteins that regulate mitochondrial functions,[11] those that regulate mitochondrial fission [dynamin-like protein 1 (Dlp1; official name *DNM1L*), fission 1], and fusion [(mitofusins 1 and 2 and optic atrophy 1)] are particularly interesting. Models of PD show dramatic effects in mitochondrial morphological features, which can be rescued by altering expression of these proteins.[12,13] Our previous study profiled the mitochondrial fraction of the SNpc in healthy control and PD patients and identified specific alterations in expression of Dlp1, but not other mitochondrial fission and fusion proteins in PD brains,[14] suggesting Dlp1 plays a role in PD pathogenesis. However, the cellular origin and consequences of decreased Dlp1 expression remain to be fully elucidated.

A recent investigation found that Dlp1 potentially interacts with the glutamate transporter 1 (GLT-1; official name *SLC1A2*),[15] which is specifically expressed by astrocytes,[16] implicating this cell type in Dlp1-mediated pathogenic effects. In theory, disrupting astrocyte regulation of extracellular glutamate [also a function of the glutamate aspartate transporter (GLAST; official name *SLC1A3*[17])] could result in excessive extracellular glutamate. This excess glutamate could prolong the opening of neuronal N-methyl-D-aspartate (NMDA) receptors,[18] resulting in excessive Ca^{2+} entry and, ultimately,

Supported by NIH grants AG033398, ES004696-5897, ES007033-6364, ES016873, ES019277, NS057567, NS060252, NS062684-6221, NS082137 (J.Z.), and T32 ES007032 (J.G.H.), and National Institute of Environmental Health Sciences grant T32 ES015459 (T.J.C. and T.S.).

Disclosures: None declared.

http://dx.doi.org/10.1016/j.ajpath.2014.10.022

neuronal death. Indeed, this phenomenon of excitotoxicity has been implicated in PD and animal models of PD,[19,20] as well as in other neurodegenerative diseases.

To test the hypothesis that decreased astrocytic Dlp1 expression contributes to neurodegeneration in PD, we measured astrocytic and neuronal Dlp1 expression, in the SNpc and cortex, in both PD and healthy control patients and explored the molecular mechanisms related to astrocytic dysfunction resulting from decreased Dlp1 expression.

Materials and Methods

Isolation of Mitochondria from Human Tissue

Mitochondria from frozen SNpc of healthy control and PD patients were isolated, as previously described,[14] and resuspended in a buffer of 6 mol/L urea, 0.05% SDS, 5 mmol/L EDTA, and 50 mmol/L Tris-HCl (pH. 8.5). Protein concentrations were determined by bicinchoninic acid assay (Pierce, Rockford, IL), and 10 μg of protein was used for Western blot analysis.

Western Blot Analysis

Transfected astrocytes were collected in radioimmunoprecipitation assay buffer, sonicated on ice, and centrifuged at 15,000 × *g* for 10 minutes. The resulting supernatant was collected as astrocyte protein sample, and concentration was determined by bicinchoninic acid assay. Protein from human tissue or astrocytes was added to Lammeli solution (Biorad, Hercules, CA). For Dlp1 detection, Lammeli solution had 2-mercaptoethanol and was boiled for 5 minutes. For GLT-1 or GLAST detection, 2-mercaptoethanol and boiling were omitted. Proteins were separated by SDS-PAGE and transferred onto polyvinylidene difluoride. Membranes were blocked with 5% milk in Tris-buffered saline and Tween-20 (TBS-T). Primary antibodies were diluted in blocking buffer [mouse anti-Dlp1, dilution 1:2000 (BD Biosciences, San Jose, CA), mouse anti-excitatory amino-acid transporter (EAAT2), dilution 1:1000 (Millipore, Billerica, MA), and rabbit anti-EAAT1, dilution 1:1000 (Cell Signaling, Beverly, MA)]. Horseradish peroxidase–conjugated secondary antibodies diluted in 3% bovine serum albumin [BSA; anti-mouse or anti-rabbit, dilution 1:20,000 (Sigma-Aldrich, St. Louis, MO)] were used to detect labeled proteins, with enhanced chemiluminescence (GE Healthcare, Little Chalfont, UK). Membranes were reblotted for ß-actin [mouse, dilution 1:4000 (Abcam, Cambridge, UK)] as a loading control. Intensity for Dlp1 in mitochondrial extracts was measured using Quantity One (Biorad). Each value was normalized to the average intensity of Dlp1 from control patients.

Tissue Staining

Fixed and paraffin-embedded tissue sections were deparaffinized by washing 4× for 10 minutes in xylene and 2× for 5 minutes in 50% xylene/50% ethanol. Tissue was rehydrated by washing 2× for 5 minutes in 100% ethanol, 3× for 1 minute in 95%, 70%, and 50% ethanol, rinsed in deionized water, and washed 2× for 5 minutes in phosphate-buffered saline (PBS). Tissue was heated (≥100°C) in 10 mmol/L citric acid (pH 6.0) for 15 minutes, cooled for 30 minutes at room temperature (25°C), and washed 3× for 10 minutes with TBS-T. Tissue was blocked overnight in 5% normal goat serum (NGS), 2% BSA, and 0.25% Triton X-100, made in TBS-T. Tissue was incubated with primary antibodies in blocking solution overnight [rabbit anti-tyrosine hydroxylase, dilution 1:500 (Pel-Freez Biologicals, Rogers, AR), mouse anti-Dlp1, dilution 1:100 (BD Biosciences), rabbit anti–mitogen-activated protein (MAP) 2, dilution 1:200 (Millipore), and rabbit anti-glial fibrillary acidic protein (GFAP), dilution 1:500 (Dako, Golstrup, Denmark)]. After incubation with primary antibodies, tissue was washed with 5% NGS and 2% BSA in TBS-T 3× for 10 minutes, and incubated with secondary antibodies conjugated with Alexa Fluor 488 or 568 (dilution 1:500; Life Technologies, Carlsbad, CA) in 5% NGS and 2% BSA, made in TBS-T, overnight. After incubation with secondary antibodies, tissue was washed 3× for 10 minutes in TBS-T, followed by rocking in 0.3% Sudan Black in 70% ethanol for 30 minutes. Tissue was rinsed twice in 70% ethanol, washed 3× for 10 minutes in TBS-T, and mounted with Vectashield with DAPI (Vector Laboratories, Burlingame, CA).

Fluorescence Staining

Cells were fixed in 4% paraformaldehyde for 30 minutes at room temperature, washed 2× for 5 minutes with PBS, and blocked in 4% NGS, 1% BSA, and 0.4% Triton X-100 for 1 hour at room temperature. Primary antibodies were diluted in blocking buffer and incubated overnight at 4°C . Co-cultured cells were incubated with rabbit anti-tyrosine hydroxylase (TH; dilution 1:200; Millipore) and mouse anti-MAP2 (dilution 1:200; Abcam). Astrocytes transfected with 488-tagged siRNA were incubated with mouse anti–GLT-1 [dilution 1:200; a kind gift from Dr. Jeffry Rothstein (Johns Hopkins Medical School, Baltimore, MD)] or rabbit anti-EAAT1 (dilution 1:200; Abcam), each with chicken anti-GFAP (dilution 1:500; Millipore). Astrocytes fixed after mitochondrial imaging were stained with rabbit anti-GFAP. Cells were washed 3× for 5 minutes with 0.1% Tween-20 in PBS and incubated with secondary antibodies conjugated with Alexa Fluor 488, 568, or 633 diluted 1:500 (488 and 568) or 1:100 (633) in 0.3% Triton X-100 in PBS for 1 hour at room temperature, followed by washing 3× for 5 minutes with 0.1% Tween-20 in PBS. Stained cells were mounted with Vectashield with DAPI.

Astrocyte and Astrocyte/Neuron Cultures

Animal use was approved by the Institutional Animal Care and Use Committee of the University of Washington

(Seattle, WA). Primary cortical astrocytes were prepared from postnatal day 0 to 1 Sprague-Dawley rats. Cortices were isolated and cleaned of blood vessels and meninges in cold dissecting media (Dulbecco's modified Eagle's medium F12; Life Technologies). Tissue was digested for 30 minutes at 37°C in Dulbecco's modified Eagle's medium F12 with 0.5 mmol/L EDTA, 0.2 mg/mL L-cysteine, 15 U/mL papain (Worthington Biochemical, Lakewood, NJ), and 10 μg/mL DNase (Worthington Biochemical) (10-mL digestion media per three brains). After digestion, cortical tissue was washed three times with culture media [Dulbecco's modified Eagle's medium F12 supplemented with 10% fetal bovine serum and 1% penicillin/streptomycin (Corning, Tewksbury, MA)]. After washing, cortices were triturated with a fire-polished Pasteur pipette in 10 mL of culture media. Tissue was allowed to settle, and the supernatant was passed through a cell strainer (pore size, 100 μm). The remaining tissue was triturated again in 5 mL of culture media, passed through a strainer, and combined with the previous 10 mL of triturated cells. The resulting cells were seeded in culture media, into vented 75-cm^2 flasks coated with poly-D-lysine, two brains per flask. Culture medium was changed 24 hours later, and astrocytes were maintained at 37°C, 5% CO_2, until they reached confluence (9 to 10 days), at which point they were plated for use.

Flasks containing confluent astrocyte cultures were gently shaken to remove microglia, washed once with PBS, and incubated with 0.25% trypsin EDTA at 37°C for approximately 5 minutes. Cells were washed with an equal volume of media, collected into a 50-mL conical tube, and centrifuged at 1900 × *g* for 10 minutes at room temperature. The resulting pellet was resuspended to a final volume of 10 mL per flask collected, and counted using a hemocytometer. Cells were plated onto glass coverslips (for co-culture, 25×10^4 cells per coverslip) or into 6-well plates (for Western blot analysis, 10×10^5 cells per well). Cultures were at least 95% GFAP positive.

Astrocytes were transfected with Lipofectamine 2000 (Life Technologies), according to the manufacturer's instructions, with slight modifications. Control or Dlp1 siRNA (Qiagen, Venlo, the Netherlands), 2 pmol per well for 24-well plates or 200 pmol per well for 6-well plates, was used. Astrocytes were maintained in media and collected at times similar to when media changes and glutamate treatment occurred for co-cultures, respectively (described later). Similar plating and transfection with 488-tagged siRNA was performed on astrocytes to assess GLT-1 and GLAST localization. Transfection efficiency differed depending on the technique for which it was used. When plated onto glass coverslips (as in astrocyte-neuron co-cultures) or for Western blot analysis, transfection with siRNA efficiency was between 60% and 70%, assessed using Western blot analysis for Dlp1. When plated for Ca^{2+} imaging (35-mm glass-bottom dishes, same volumes as 6-well plates), efficiency was approximately 95%, assessed by imaging 488-tagged siRNA after transfection (Dlp1 knockdown by 488-tagged siRNA was validated with Western blot analysis). When plated for mitochondrial imaging (described later), efficiency was <50%, assessed by imaging 488-tagged siRNA after transection; however, staining for MnSOD, to observe mitochondrial morphological characteristics, in plates transfected similarly to those for Ca^{2+} imaging, showed the same morphological phenotype after Dlp1 knockdown.

To prepare co-cultures, timed pregnant Sprague-Dawley rats (Harlan Animal Research Labs, Indianapolis, IN) were anesthetized with carbon dioxide. Pups (embryonic days 16 to 18) were removed, and the brains were placed in cold neuronal dissection media [Neurobasal A supplemented with B27 and 0.5 mmol/L L-glutamine (Life Technologies)]. Ventral mesencephalons were dissected from the brains and digested for 15 minutes at 30°C in 12 mL Hibernate A without calcium chloride (BrainBits, Springfield, IL), 0.5 mmol/L L-glutamine, 15 U/mL papain, and 17 μg/mL DNase. Tissue was washed three times with neuronal dissection media and triturated in 2 mL of the same media with a fire-polished Pasteur pipette. Tissue was allowed to settle, and the supernatant was passed through a cell strainer (pore size, 100 μm). Trituration and cell straining were repeated twice more. Cells were spun at 200 × *g* for 5 minutes at room temperature. The resulting pellet was resuspended in neuronal media (Neurobasal A supplemented with B27, 2 mmol/L L-glutamine, and 1% penicillin/streptomycin) and counted using a hemocytometer. Cells (12.5×10^4 per well) were plated onto transfected astrocytes in neuronal media. Neurons were allowed to grow for 8 days before treatment.

Live and Immunofluorescence Imaging

To quantify Dlp1 in tissue, Z-series images were captured for 15 randomly selected fields of GFAP-positive astrocytes and 20 fields of MAP2-positive (and neuromelanin negative for SNpc) or TH-positive neurons in each region. A single image from the middle section was selected to quantify Dlp1 intensity. Astrocytes in the SNpc were imaged at magnification ×100 using a Biorad LS2000 laser-scanning confocal microscope. All other imaging was done at ×60 magnification using a Nikon Eclipse Ti microscope (Nikon Instruments Inc., Melville, NY). Microscope settings were kept the same for each cell type from each region using NIS-Elements software version 3.2 (Nikon Instruments Inc.). For quantification, each value was normalized to the average Dlp1 intensity of the control patients for the cell type and region being analyzed. All image analysis was performed using ImageJ software version 10.2 (NIH, Bethesda, MD) and NIS-Elements software. Images were deconvolved, and Dlp1 intensity was measured by manually tracing cells, selecting a region of interest, and calculating the mean fluorescence of the region. Image capture and quantification were done without knowledge of case diagnosis.

Astrocytes used for intracellular or mitochondrial Ca^{2+} imaging were plated onto 35-mm dishes with a 14-mm glass coverslip (MatTek, Ashland, MA), coated with poly-D-lysine. Cells (25×10^4 per well) were plated onto the coverslips at a final volume of 500 μL, and returned to 37°C for 2 hours to allow cells to adhere. After 2 hours, medium was added to a final

volume of 2 mL. Astrocytes were transfected as with 6-well plates. For transfection of Mito-DsRed2 plasmid (Clontech, Mountain View, CA) and 488-tagged siRNA, 6-well plasmid instructions were followed using 4 μg plasmid and 100 pmol siRNA per plate.

To measure astrocyte intracellular or mitochondrial Ca^{2+} responses to glutamate, cells were loaded with Oregon Green 488 1,2-bis (aminophenoxy) ethane-N,N,N′,N′-tetraacetic acid acetoxymethyl ester or rhod-2 AM, respectively (Life Technologies). The dye (50 μg) was shaken in 10 μL of 15% Pluronic F-127 in dimethyl sulfoxide (Life Technologies) at 4°C for 30 minutes. Dye was diluted to a final concentration of 4 μmol/L in neuronal media and incubated with the cells for 30 minutes at 37°C (Oregon Green) or room temperature (rhod-2 AM). Cells were then either washed 3× for 10 minutes with neuronal media and imaged for total intracellular Ca^{2+} after the third wash or washed 3× with neuronal media and incubated at 37°C for 1 hour before imaging for mitochondrial Ca^{2+}.

All Ca^{2+} imaging was performed using a Nikon Eclipse Ti microscope and NIS-Elements Software at ×60 magnification and 37°C. Fields of cells were randomly selected, and fluorescent intensity was measured every 200 milliseconds (total intracellular Ca^{2+}) or 1 second (mitochondrial Ca^{2+}). Cells were imaged for 2 minutes, at which point glutamate was added to a final concentration of 100 μmol/L, and responses were recorded for approximately 8 minutes after stimulation. Three to four plates were used per replicate. Response data were exported to Microsoft Excel (Redmond, WA) and quantified. Intracellular Ca^{2+} responses were categorized as response types. Types 1 and 2 were defined by large increases of intracellular Ca^{2+}. Type 1 responses lasted >60 seconds, and type 2 responses were 60 seconds or less. Types 3 and 4 were defined as having Ca^{2+} oscillations, with type 3 having lower frequency (<0.19 Hz) and type 4 having greater frequency (at least 0.19 Hz). Proportions of responses were calculated for each replicate. Mitochondrial Ca^{2+} responses were calculated by measuring the change in fluorescence from baseline and dividing by baseline fluorescence. Values for each cell were calculated and used for analysis.

Mitochondrial Measurements

To assess mitochondrial movement, astrocytes were maintained in medium identical to that used for astrocyte/neuron co-cultures. Three random fields of astrocytes positive for the siRNA (green) and Mito-DsRed2 plasmid were selected for each plate in each replicate and imaged at 37°C. Images were captured every 5 seconds for 5 minutes. Movement was assessed by measuring the net distance moved by mitochondria within the processes toward (retrograde) or away (anterograde) from the astrocyte cell body during the 5-minute span. Measurements for mitochondria movement in each direction were averaged for each cell.

After imaging, astrocytes were fixed and stained with GFAP to assess mitochondrial length and morphological characteristics. Ten random fields were selected, and Z-series images were captured. Files were deconvolved, and maximum intensity projections were generated. Mitochondria within the processes were analyzed because individual mitochondria were more easily resolved than those in the cell body. For astrocytes with Dlp1 knocked down, it was not uncommon for elongated mitochondria to continue into the cell body. In this event, the process was cropped at the cell body and mitochondria were analyzed as if the point where they reached the cell body was the end. The perimeters of mitochondria were selected using the software and, from this, length and area were automatically calculated. To assess density, the number of mitochondria in the process was

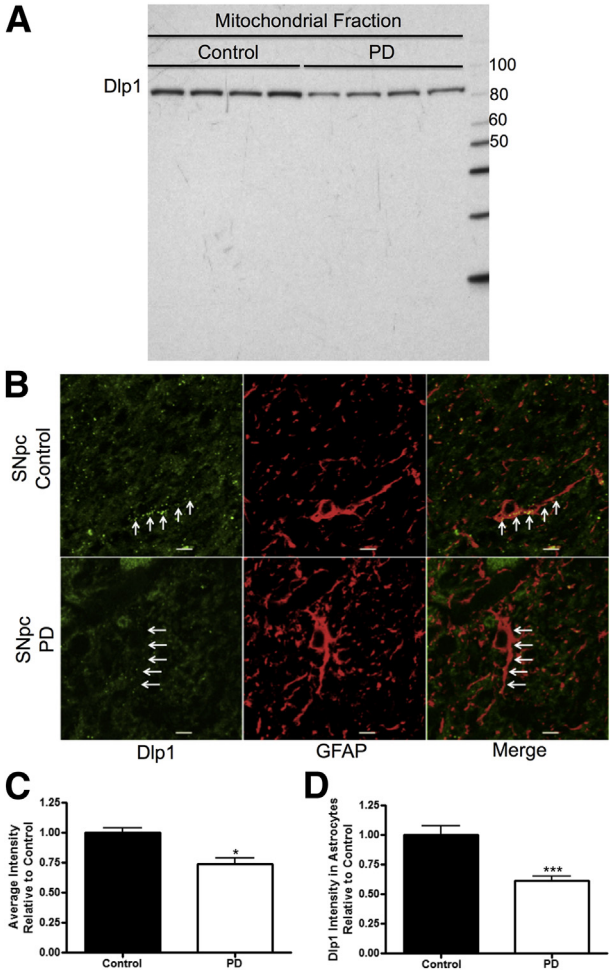

Figure 1 Dynamin-like protein 1 (Dlp1) expression is decreased in the substantia nigra pars compacta (SNpc) of Parkinson disease (PD) patients. Western blot analysis (**A**) and densitometry (**C**) of the mitochondrial-enriched fraction of the SNpc from control patients ($N = 4$) and PD patients ($N = 4$) show decreased Dlp1 in mitochondria-enriched tissue (the units for molecular weight markers on the right of the Western blot are kDa). **B:** Fluorescent staining of Dlp1 (green) and glial fibrillary acidic protein (GFAP; red) in the SNpc of control patients and PD patients. **Arrows** point at Dlp1 and GFAP colocalization. **D:** Quantification of Dlp1 intensity in astrocytes from the SNpc of control ($N = 6$ cases, 109 cells) and PD patients ($N = 6$ cases, 118 cells). Data are presented as means ± SEM. $^*P < 0.05$, $^{***}P < 0.001$ by two-sided unpaired t-test. Scale bar = 20 μm (**B**).

counted and divided by the area of the process. For each measurement, the values for individual cells were averaged.

Glutamate Treatment of Astrocyte-Neuron Co-Cultures

To assess astrocyte protection against excitotoxic environments, co-cultures were gently shaken to remove residual microglia and treated with normal neuronal media (No Treatment), neuronal media supplemented with 10 μmol/L glutamate (10 μmol/L Glu), or neuronal media supplemented with 10 μmol/L each of glutamate and MK-801 (10 μmol/L Glu + MK-801; Sigma) for 10 minutes. Treatments were replaced with normal neuronal media and allowed to recover for 1 hour, at which point co-cultures were fixed and stained.

H^3-D-Aspartate Uptake

Uptake assays were performed on co-cultures in duplicate, similar to published protocols.[21] Cells were washed twice with warm Krebs-Ringer solution (16 mmol/L sodium phosphate, 119 mmol/L NaCl, 4.7 mmol/L KCl, 1.8 mmol/L $CaCl_2$, 1.2 mmol/L $MgSO_4$, 1.3 mmol/L EDTA, and 5.6 mmol/L glucose; pH 7.4). After the second wash, cells were incubated with Krebs-Ringer solution with H^3-D-aspartate (1.3 μmol/L; 0.03 μCi/mL, specific activity 1 mCi/mL; American Radiolabeled Chemicals, St. Louis, MO) at 37°C for 10 minutes. Co-cultures were washed three times with ice-cold Krebs-Ringer solution. After the third wash, cells were rocked in 1N NaOH for 30 minutes at room temperature. The resulting solutions were collected in scintillation fluid and measured using a scintillation counter. For each replicate, H^3 measurements were averaged for each group (siRNA) and normalized to the value for co-cultures where control siRNA was transfected into astrocytes.

Measurement of Neurons

A Nikon Eclipse 80i microscope (Nikon Instruments Inc.) was used to capture images for assessing viability of neurons in response to treatments. Ten random fields of TH-positive neurons and their processes were captured and traced using Neurolucida (MBF Bioscience, Williston, VT) to assess average process (neurite) length and number of branch points. To assess the viability of non-dopaminergic (non-DAergic) neurons in response to treatments, five random fields of MAP2-positive and TH-negative neurons were captured and similarly traced. Cells from each replicate were normalized to the average length or number of branch points of neurons from No Treatment control siRNA co-cultures.

Statistical Analysis

Statistical analysis was performed using GraphPad Prism version 6 (San Diego, CA). Differences between groups were assessed using two-sided unpaired *t*-tests, two-way analysis of variance with Bonferroni correction, or two-sample Kolmogorov-Smirnov test to assess if the groups were equal, and are specified in each figure legend.

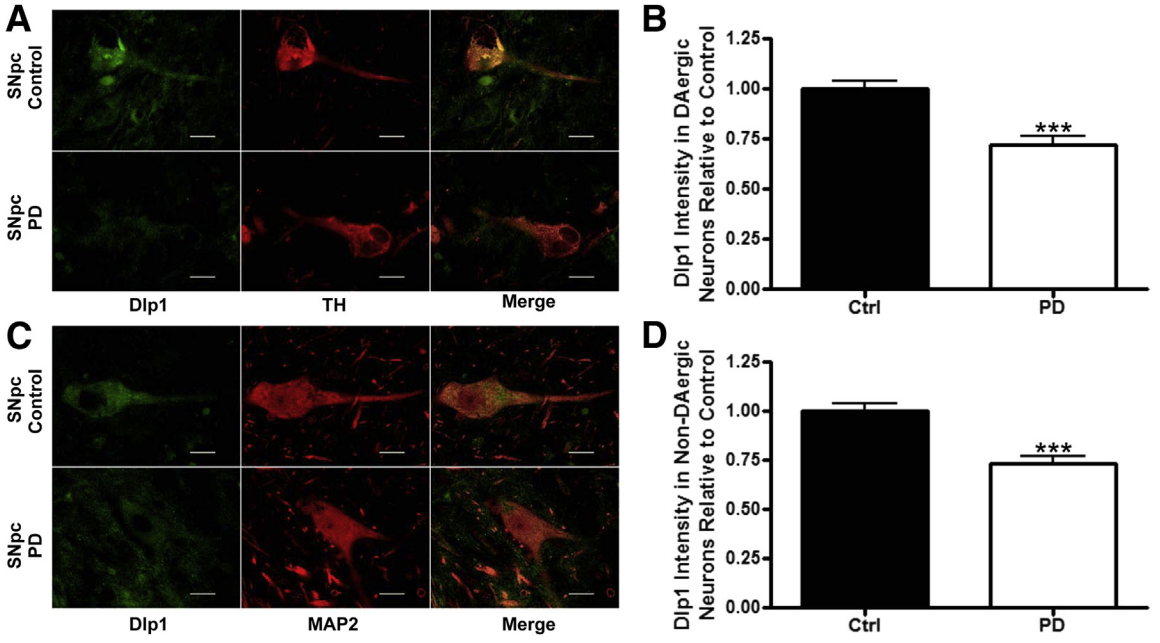

Figure 2 Dynamin-like protein 1 (Dlp1) expression is decreased in neurons in the substantia nigra pars compacta (SNpc) of Parkinson disease (PD) patients. **A:** Fluorescent staining of Dlp1 (green) and tyrosine hydroxylase (TH; red) in the SNpc of control and PD patients. **B:** Quantification of Dlp1 intensity in dopaminergic (DAergic) neurons from SNpc of control (Ctrl; $N = 6$ cases, 253 cells) and PD patients ($N = 6$ cases, 143 cells). **C:** Fluorescent staining of Dlp1 and mitogen-activated protein (MAP) 2 (red) without neuromelanin in SNpc of control and PD patients. **D:** Quantification of Dlp1 intensity in non-DAergic neurons from control ($N = 6$ cases, 185 cells) and PD patients ($N = 6$ cases, 175 cells). Data are presented as means ± SEM. $***P < 0.001$ by two-sided unpaired *t*-test. Scale bar = 20 μm (**A** and **C**).

Significance was defined as $P < 0.05$. All bar graphs are presented as means ± SEM.

Results

Dlp1 Expression Decreases in Astrocytes and Neurons from PD Patients

Previously, by using mass spectrometry and pooled SNpc samples, we found that PD patients had lower Dlp1 expression compared to healthy controls.[14] Our goal was to demonstrate the previous findings in individual PD cases with a different technology. Therefore, the SNpc mitochondrial fraction from four PD and four control patients was examined via Western blot analysis with an anti-Dlp1 antibody. In agreement with our previous work,[14] Dlp1 protein expression was significantly lower in PD patients (Figure 1, A and C).

The astrocytic Dlp1 expression levels were measured in the SNpc of PD and control patients by immunofluorescence. We found an obvious decrease of astrocytic Dlp1 expression in PD patients (Figure 1, B and D). In addition, neuronal Dlp1 expression was measured in DAergic (Figure 2, A and B; information for human tissue is in Table 1) and non-DAergic neurons in the SNpc of PD patients and controls in Figure 2, C and D. Again, Dlp1 immunofluorescence was significantly decreased in both DAergic and non-DAergic neurons (Figure 2, A–D). Next, we asked whether the observed decrease in Dlp1 expression also occurred in histologically normal cortex from PD patients (ie, PD patients at a relatively early stage, without apparent cortical neurodegeneration). Remarkably, Dlp1 expression was decreased in both cell types (Figure 3, A–D).

Dlp1 Affects Astrocytic Mitochondrial Morphological Characteristics and Localization

To understand the biological effects of decreased Dlp1 expression in astrocytes, we performed Dlp1 (*Dnm1l*) knockdown by siRNA in primary cortical rat astrocytes (Figure 4B). No change was observed in expression levels of other mitochondrial fission/fusion proteins (optic atrophy 1, mitofusins 1 and 2, and fission 1) assessed by Western blot analysis (data not shown). Astrocytes cotransfected with 488-tagged siRNA and a Mito-DsRed2 plasmid, to observe mitochondria, were stained for GFAP. Knockdown of Dlp1 in astrocytes resulted in dramatic morphological changes primarily characterized by an elongated, fused mitochondrial network (Figure 4A), similar to what has been observed in other cell types.[12,22] Mitochondria located in astrocyte processes had clear morphological features and, therefore, were used to quantitatively compare morphological and localization differences after Dlp1 knockdown. Mitochondria in astrocytes transfected with Dlp1 siRNA were significantly longer than those in astrocytes transfected with non-specific (control) siRNA (Figure 4, A and B). In addition, the area and perimeter of mitochondria were significantly larger in astrocytes after Dlp1 knockdown (Figure 4, A, C, and D). Furthermore, there were fewer mitochondria within astrocyte processes after Dlp1 knockdown (Figure 4E), indicating that knockdown of Dlp1 resulted in extensive fusion of mitochondria. Live cell imaging was used to measure net anterograde and retrograde mitochondrial movement to determine whether Dlp1 knockdown altered mitochondrial motility (Figure 5A). The net distance traveled by mitochondria, in each direction, was greater in astrocytes transfected with control siRNA compared to astrocytes transfected with Dlp1 siRNA (Figure 5, B and C, and Supplemental Movies S1 and S2). This evidence suggests that Dlp1 plays a significant role in astrocytic regulation of the morphological features, localization, and motility of their mitochondria.

Table 1 Clinical Data for PD and Control Cases Used for SNpc and Frontal Cortex Cases

Case no.	Diagnosis	Region	Age (years)	Sex	PMI (hours: minutes)
1	Ctrl	SNpc	55	M	9:30
2	Ctrl	SNpc	70	F	6:00
3	Ctrl	SNpc	79	M	7:50
4	Ctrl	SNpc	78	M	4:00
5	Ctrl	SNpc	79	F	2:30
6	Ctrl	SNpc	81	M	7:30
7	PD	SNpc	57	M	17:45
8	PD	SNpc	82	F	11:00
9	PD	SNpc	81	M	6:30
10	PD	SNpc	80	M	6:30
11	PD	SNpc	58	F	>24
12	PD	SNpc	73	M	3:50
13	Ctrl	FC	78	M	4:00
14	Ctrl	FC	78	M	6:00
15	Ctrl	FC	81	M	5:30
16	Ctrl	FC	81	M	6:00
17	Ctrl	FC	82	F	3:30
18	Ctrl	FC	91	F	11:00
19	PD	FC	73	M	3:50
20	PD	FC	78	M	5:00
21	PD	FC	81	M	6:30
22	PD	FC	82	F	11:00
23	PD	FC	91	F	4:10
24	PD	FC	89	F	<12

All cases were devoid of cortical neurofibrillary tangles.

F, female; M, male; Ctrl, control patient; FC, frontal cortex; PD, Parkinson disease; PMI, post-mortem interval; SNpc, substantia nigra pars compacta.

Astrocytic Dlp1 Protects Neurons from Excessive Glutamate

A co-culture system of rat astrocytes (with or without Dlp1 siRNA) and neurons from the ventral mesencephalon was used to determine whether decreased astrocytic Dlp1 impairs astrocytic protection of neurons from the excitotoxic effects of excess glutamate. When DAergic neurons were

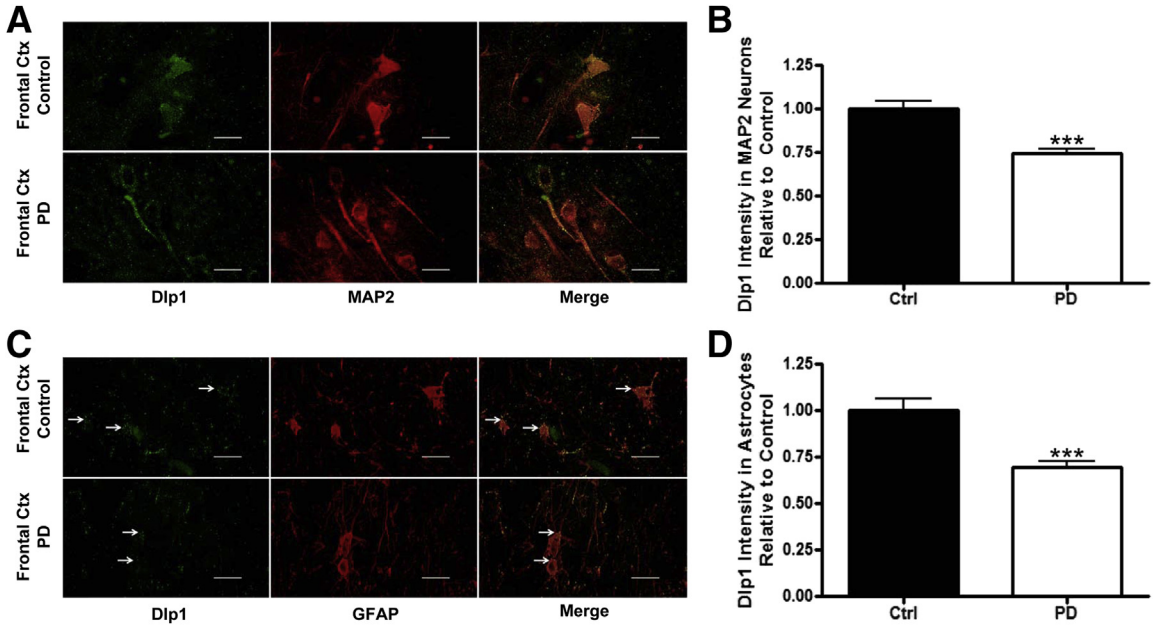

Figure 3 Dynamin-like protein 1 (Dlp1) expression is decreased in neurons and astrocytes in the frontal cortex of Parkinson disease (PD) patients. **A:** Fluorescent staining of Dlp1 (green) and mitogen-activated protein (MAP) 2 (red) in frontal cortex of control and PD patients. **B:** Quantification of Dlp1 intensity in neurons from control ($N = 6$ cases, 357 cells) and PD patients ($N = 6$ cases, 385 cells). **C:** Fluorescent staining of Dlp1 and glial fibrillary acidic protein (GFAP; red) in frontal cortex from control and PD patients. **Arrows** point at Dlp1 and GFAP colocalization. **D:** Quantification of Dlp1 intensity in astrocytes from control ($N = 6$ cases, 230 cells) and PD patients ($N = 6$ cases, 229 cells). Data are presented as means ± SEM. $***P < 0.001$ by two-sided unpaired *t*-test. Scale bar = 20 μm (**A** and **C**). Ctx, cortex.

co-cultured with astrocytes transfected with control siRNA, 10 μmol/L glutamate did not affect DAergic neurite length or the number of branch points (highlighted by TH-positive) (Figure 6, A–C). Conversely, when DAergic neurons were co-cultured with astrocytes transfected with Dlp1 siRNA (decreased Dlp1 expression), the addition of 10 μmol/L glutamate decreased DAergic neurite length and the number of branch points. The administration of the NMDA receptor antagonist, MK-801, at the time of glutamate treatment prevented these morphological changes (Figure 6, A–C). This evidence indicates that astrocytic Dlp1 promotes the protection of DAergic neurons from glutamate excitotoxicity.

Similar measurements were performed on non-DAergic MAP2-positive neurons to assess if this effect was specific to TH-positive neurons. As was the case with TH-positive neurons, treatment with 10 μmol/L glutamate did not affect neurite length or branch point number of non-DAergic neurons in co-culture with astrocytes transfected with control siRNA (Figure 6, B–D). However, in non-DAergic neurons co-cultured with astrocytes transfected with Dlp1 siRNA, the addition of 10 μmol/L of glutamate resulted in decreased neurite length and branch point number. Again, this effect could be prevented by the addition of MK-801 (Figure 6, B–D). These observations suggest that decreased astrocytic Dlp1 expression impairs their ability to protect neighboring neurons from the harmful effects of excess glutamate. Astrocytic neuronal protection should be dependent on proper function of the glutamate transport system. Therefore, we assessed the uptake of H^3-D-aspartate to investigate whether the loss of astrocytic Dlp1 impaired the glutamate transport system. The cultures with astrocytes transfected with Dlp1 siRNA absorbed less H^3-D-aspartate than cultures with astrocytes treated with control siRNA (Figure 6E). This result supports the hypothesis that astrocytic glutamate transport is impaired by decreased Dlp1 expression.

Because Dlp1 is reported to interact with GLT-1,[15] we investigated whether decreased Dlp1 expression alters the expression and/or localization of GLT-1. Western blot analysis of astrocytic GLT-1 showed no change in protein expression when transfected with Dlp1 siRNA (Supplemental Figure S1A). We immunofluorescently stained GLT-1 in astrocytes transfected with Dlp1 siRNA to observe astrocytic GLT-1 localization. Again, the localization of GLT-1 did not appear to be affected by Dlp1 expression (Supplemental Figure S1B). In similar experiments, we examined the other major astrocytic glutamate transporter, GLAST. Similarly, Dlp1 siRNA did not interfere with GLAST expression or localization (Supplemental Figure S1, C and D). Therefore, given that protein knockdown in these experiments was comparable to those from the co-culture experiments (approximately 60% to 70%), alterations to the glutamate transport system caused by astrocytic Dlp1 knockdown did not occur through changes in the expression or localization of the major astrocytic glutamate transporters.

Dlp1 Affects Astrocytic Regulation of Calcium Entry

Cultured astrocytes were imaged in the presence of the Ca^{2+}-sensitive dye Oregon Green 1,2-bis (aminophenoxy)

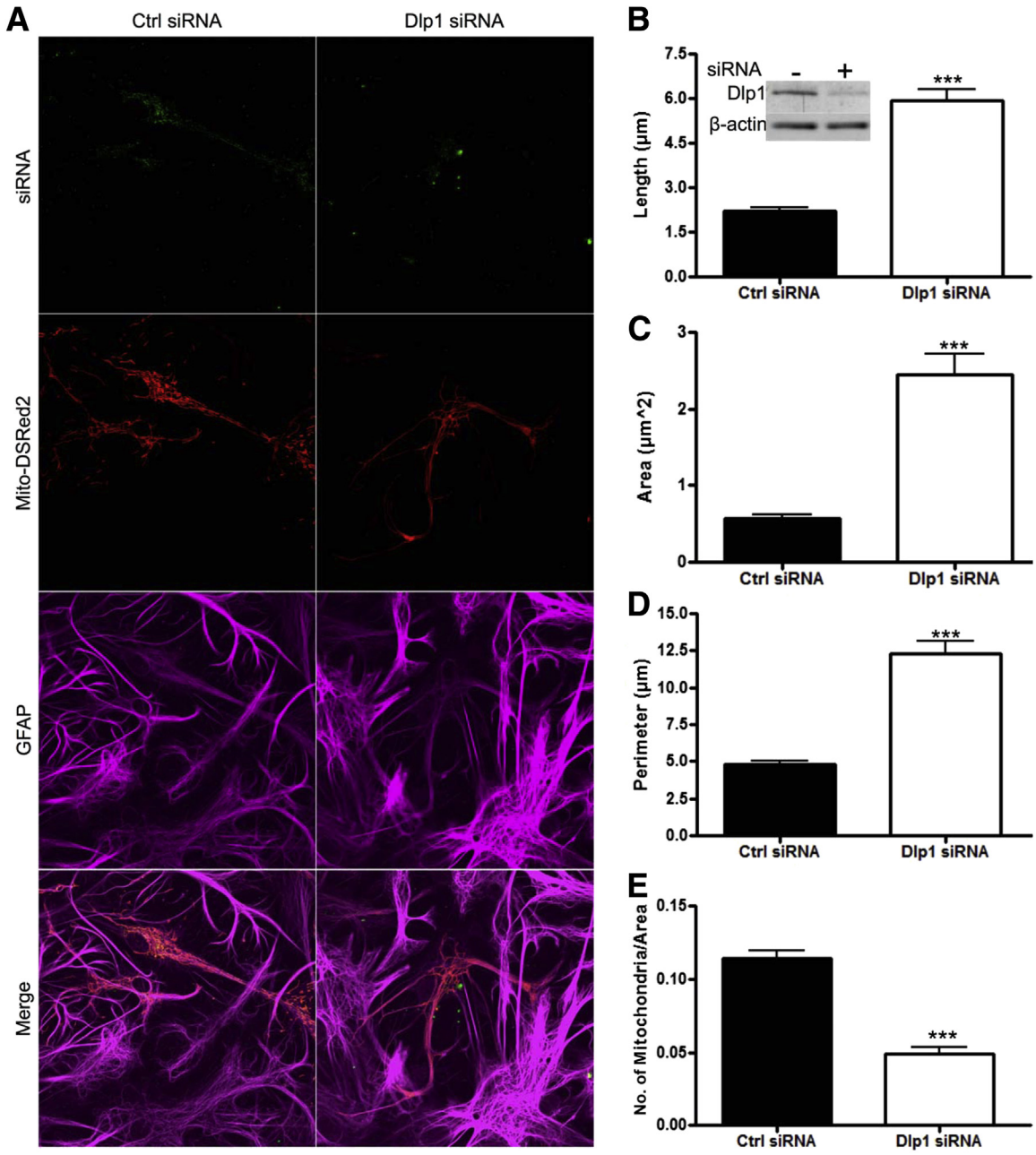

Figure 4 Knockdown of dynamin-like protein 1 (Dlp1; *DNM1L*) in astrocytes results in elongation and interconnection of mitochondria. **A:** Representative images of rat astrocytes transfected with non-specific [control (ctrl)] siRNA or siRNA targeting Dlp1, each labeled with a 488 tag, and a Mito-DsRed2 plasmid to observe mitochondria. Cells that were positively transfected with both siRNA and Mito-DsRed2 were identified by the presence of green and red fluorescence. Western blot analysis (**inset**, **B**) confirmed siRNA decreased Dlp1 expression. Length (**B**), area (**C**), perimeter (**D**), and density (**E**) of mitochondria from processes of transfected astrocytes ($N = 5$ replicates; 50 to 56 cells per group). Data are presented as means ± SEM. $^{***}P < 0.001$ by two-sided unpaired *t*-test.

ethane-N,N,N′,N′-tetraacetic acid to determine whether decreased Dlp1 alters astrocytic intracellular Ca^{2+} responses to extracellular glutamate. Astrocyte responses to glutamate could be categorized into four general categories. Under control conditions, a minority of cells responded with a single, large increase in intracellular Ca^{2+}, which could be either prolonged (taking >60 seconds to return to baseline) or attenuated (taking 60 seconds or less to return to baseline). We categorized these cell responses as types 1 and 2, respectively (Figure 7A). The remaining cells responded with intracellular Ca^{2+} oscillations, and we categorized these cell responses by oscillation frequency. Type 3 responses were characterized by less frequent oscillations (<0.19 Hz), and type 4 responses were characterized by more frequent oscillations (≥0.19 Hz) (Figure 7A). Control astrocytes demonstrated mostly type 3 and 4 responses, whereas astrocytes with decreased Dlp1 had fewer type 3 and 4 responses and significantly more type 1 responses (Figure 7B). These results indicate that astrocytic

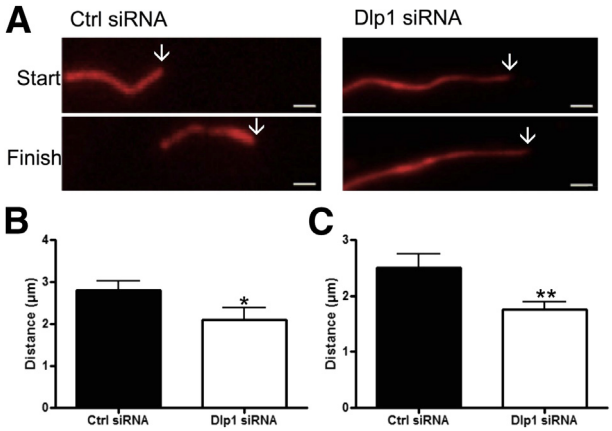

Figure 5 Knockdown of dynamin-like protein 1 (Dlp1; *DNM1L*) in astrocytes decreases mitochondrial movement. **A:** Representative image for measurements of distance for astrocytes transfected with control (ctrl) or Dlp1 siRNA. **Arrows** on the **top panels** mark beginning position, and **arrows** on the **bottom panels** mark ending position. **B:** Net movement for mitochondria away from the cell body. **C:** Net movement for mitochondria toward the cell body ($N = 6$ replicates; 28 cells per group). Data are presented as means ± SEM. $^{*}P < 0.05$, $^{**}P < 0.01$ by two-sided unpaired *t*-test. Scale bar = 1 μm (**A**).

Dlp1 knockdown results in elevated intracellular Ca^{2+} in response to glutamate.

Astrocyte responses to glutamate are initiated by an intracellular release of Ca^{2+} from the endoplasmic reticulum (ER), which precedes Ca^{2+}-induced Ca^{2+} entry from the extracellular space in a process referred to as store-operated calcium entry.[23] In addition, the binding of glutamate to ionotropic receptors allows Ca^{2+} influx from the extracellular space.[23] Therefore, the Ca^{2+} response could be driven by intracellular and/or extracellular Ca^{2+} in astrocytes with decreased Dlp1 expression. To determine how extracellular Ca^{2+} contributes to the four previously mentioned calcium responses, glutamate-induced Ca^{2+} responses were observed in the presence of the calcium chelator, EGTA. When astrocytes were bathed with 2 mmol/L EGTA, no type 1 responses were observed (Figure 7B). This result suggests that extracellular Ca^{2+} is necessary for the extended Ca^{2+} entry observed in type 1 responses. However, the pattern of Ca^{2+} waves was not different between astrocytes transfected with control or Dlp1 siRNA.

Decreased Dlp1 Impairs Mitochondrial Buffering of Extracellular Ca^{2+}

It is well-known that mitochondria buffer intracellular Ca^{2+}.[24] Given that the morphological characteristics and distribution of mitochondria are altered in astrocytes after Dlp1 knockdown, the Ca^{2+} buffering capacity of mitochondria could be limited when challenged with increased extracellular glutamate. Rhod-2 AM, a fluorometric dye sensitive to mitochondrial Ca^{2+}, was used to assess the mitochondrial buffering capacity of astrocytes transfected with control or Dlp1 siRNA in response to glutamate. Dlp1 siRNA-transfected astrocytes had lower mitochondrial peak Ca^{2+} amplitudes than those of control siRNA-transfected astrocytes (Figure 8, A and B). Therefore, knockdown of astrocytic Dlp1 impairs mitochondrial Ca^{2+} buffering in response to glutamate. In addition, the differences observed in cellular Ca^{2+} responses to glutamate were mediated by the regulation of extracellular Ca^{2+}. Therefore, mitochondrial buffering of glutamate-induced extracellular Ca^{2+} entry potentially plays a fundamental role in regulating overall cellular Ca^{2+} responses.

Discussion

Herein, we investigated the role of Dlp1 in PD pathogenesis. Dlp1 was lower in the mitochondrial fractions from the SNpc of PD patients, which was in agreement with our previous results.[14] In addition, Dlp1 was decreased in astrocytes and neurons from the SNpc of PD patients. A decrease in Dlp1 has been described in hippocampal neurons from patients with Alzheimer disease.[22] The current investigation is the first study to demonstrate decreased Dlp1 in astrocytes from PD patients. Our finding that Dlp1 is decreased in astrocytes and neurons in the frontal cortices of PD patients is also significant. Cortical regions likely play a role in the nonmotor symptoms of PD, including depression and impaired cognitive functions,[2,3] some of which occur before the onset of motor symptoms. The cortical samples examined in our study were obtained from patients without obvious cortical neurodegeneration or Lewy body disease, which occurs in late stages of PD. Therefore, decreased Dlp1 expression may represent an early event in PD neurodegeneration.

The second important finding is that decreased Dlp1 has dramatic effects on the morphological characteristics of astrocytic mitochondria. Astrocytes constitute a large proportion of cells in most brain regions, including the SNpc,[25,26] and they perform a variety of protective functions that promote neuronal survival. Decreased astrocytic Dlp1 in our *in vitro* system altered mitochondrial morphological characteristics and localization. Furthermore, Dlp1 knockdown significantly increased mitochondrial length, perimeter, and area and decreased the density of mitochondria within astrocyte processes. These results are consistent with published studies, which show alterations in mitochondrial dynamics in PD that may act through Dlp1.[12,13] Finally, Dlp1 knockdown hinders anterograde and retrograde mitochondrial movements, which leads to their abnormal localization. Thus, the astrocytic capacity for maintaining the neuronal environment may be diminished by suboptimal positioning of their mitochondria[27,28] (discussed later).

As previously mentioned, it has become increasingly recognized that astrocytes play a critical role in neuronal survival,[7] and the mechanisms by which astrocytes contribute to disease are a major area of interest. Changes in PD-related proteins in astrocytes of PD patients have implicated astrocyte

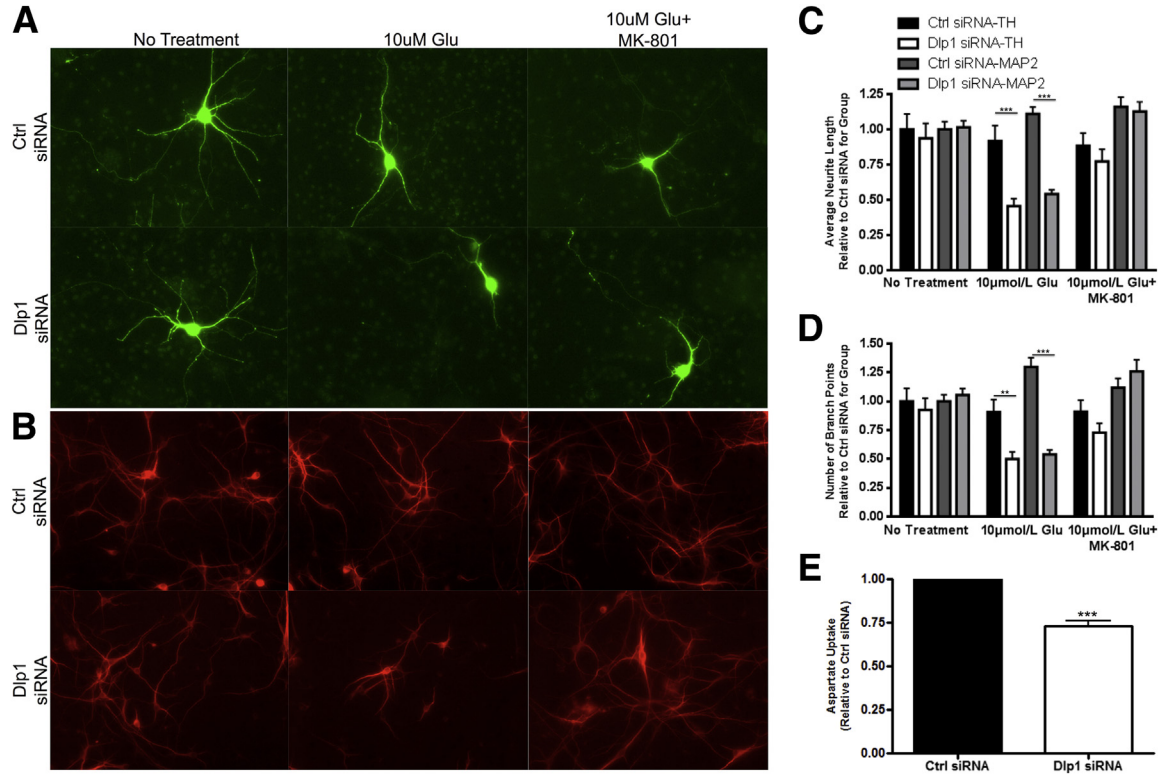

Figure 6 Astrocytic dynamin-like protein 1 (Dlp1) decreases the ability of astrocytes to protect neurons against the effects of excess glutamate. **A:** Representative images of dopaminergic (DAergic) neurons, indicated by tyrosine hydroxylase (TH) staining, co-cultured with astrocytes transfected with control (ctrl) or Dlp1 siRNA and treated as indicated. Neurons cultured with Dlp1-transfected astrocytes show shorter processes and fewer branch points after glutamate treatment. **B:** Representative images of non-DAergic neurons, indicated by mitogen-activated protein (MAP) 2 staining, cultured with astrocytes transfected and treated similar to **A**. **C:** Average neurite length for images in **A** and **B** ($n = 3$ replicates, 72 to 101 cells per group for TH-positive and approximately 650 to 800 cells per group for MAP2). **D:** Average number of branch points for images in **A** and **B** ($n = 3$ replicates). Neurite lengths and number of branch points were normalized to the average value for the No Treatment ctrl siRNA group for each replicate, and each value was used for analysis. **E:** Aspartate uptake decreases in cultures similar to **A** and **D** when astrocyte Dlp1 decreases. Data are presented as means ± SEM. $^{**}P < 0.01$, $^{***}P < 0.001$ by two-way analysis of variance with Bonferroni correction (**C** and **D**); $^{***}P < 0.001$ by two-sided unpaired *t*-test (**E**).

dysfunction as a contributing factor in disease pathogenesis.[29,30] Animal models of PD support this concept and suggest impaired astrocyte glutamate regulation as a potential mechanism.[19,31] Our study links pathologically relevant changes in astrocytic protein expression to neuronal damage due to deficiencies in the glutamate transport system. The loss of Dlp1 impairs astrocyte-mediated neuroprotection against the damaging effects of glutamate, which occur via excessive signaling through NMDA receptors on neurons. Such effects were not specific to DAergic neurons, which suggests that excitotoxicity is not the primary mechanism of specific DAergic neuronal death in PD. Gradual loss of DAergic neurons is a classic neuropathological feature found in PD. DAergic neurons from the SNpc may, therefore, be selectively vulnerable to a lifetime of small, but cumulative, excitotoxic insults or rapidly vulnerable to a large excitotoxic insult. This concept is partially supported by the finding that methylphenylpyridium ion–positive toxicity, which targets DAergic neurons, is enhanced by the application of glutamate.[32] In addition, when studied using *in vivo* toxicant-based models of PD, DAergic neuron death largely results from excessive reactive oxygen species (ROS) production and/or the inhibition of mitochondrial function. That such models can be rescued by the administration of glutamate receptor antagonists[19,20] implies that excitotoxicity plays a contributing, rather than primary, role in PD and may exacerbate the effects of another insult.

Finally, we studied the mechanism by which impaired astrocytic mitochondrial dynamics affect the glutamate transport system. We initially tested the hypothesis that impaired glutamate transport and the ensuing increased sensitivity of neurons to glutamate-mediated excitotoxicity in the presence of astrocytes with decreased Dlp1 expression resulted from altered expression or localization of astrocytic glutamate transporters, particularly GLT-1, due to separate reports that indicated Dlp1 may compartmentalize mitochondria with GLT-1.[15] Knockdown of astrocytic Dlp1 did not appear to affect expression or localization of either GLT-1 or GLAST, indicating alterations in glutamate handling occurred through a separate mechanism(s). Glutamate-induced Ca^{2+} responses were, therefore, used to assess the effects of Dlp1 knockdown on glutamate handling, because Ca^{2+} is critically important for astrocyte function, including glutamate clearance.[33,34] Indeed, astrocytic Dlp1 knockdown led to increased, prolonged Ca^{2+}

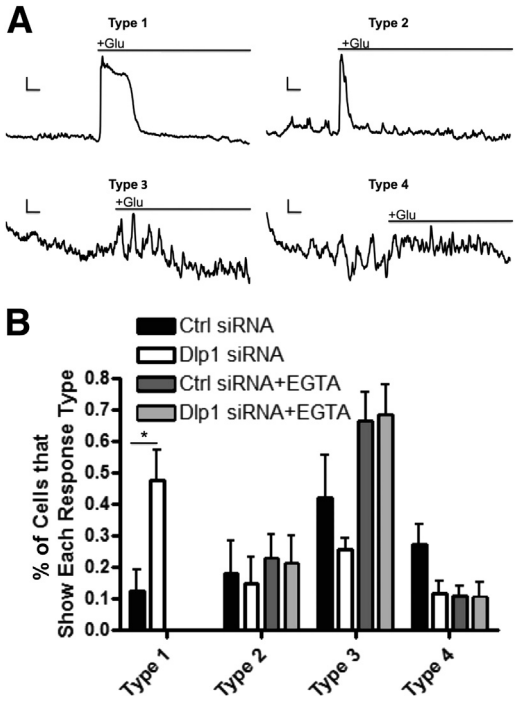

Figure 7 Intracellular Ca^{2+} is increased in response to glutamate when astrocytic Dlp1 is knocked down. **A:** Representative images of the four primary astrocyte Ca^{2+} responses to glutamate. Traces represent intracellular Ca^{2+} signals from astrocytes treated with glutamate (black line above trace). For types 1 and 2, the Y scale bar represents 500 fluorescent units (FUs) and the X scale bar represents 25 seconds. For type 3, the Y scale bar represents 50 FUs and the X scale bar represents 25 seconds. For type 4, the Y scale bar represents 30 FUs and the X scale bar represents 20 seconds. **B:** Quantification of proportions of cells shows each type of response to glutamate ($N = 5$) in normal conditions (black and white bars) or in the presence of extracellular EGTA (gray bars). The proportion of responses in each replicate was calculated, and these values were used for analysis. Astrocytes transfected with control (ctrl) siRNA tend to show response types 3 and 4, whereas those transfected with Dlp1 siRNA show a greater proportion of type 1 responses. No differences are observed between astrocytes with ctrl siRNA and Dlp1 (*DNM1L*) siRNA when EGTA is present and type 1 responses are not observed. Data are presented as means ± SEM. $*P < 0.05$ by two-way analysis of variance with Bonferroni correction.

currents in response to glutamate, which were ablated by chelation of extracellular Ca^{2+}, suggesting that astrocytic Dlp1 is important for the regulation of Ca^{2+} influxes from the extracellular space. These results may be due to the changes in mitochondrial morphological characteristics and localization. Mitochondria shape intracellular Ca^{2+} transients through their buffering capacity,[35,36] and they are transported to the sites of Ca^{2+} entry to perform efficiently.[37,38] As discussed above, knockdown of Dlp1 results in highly elongated mitochondria that cannot be transported to their destination, which results in inadequately positioned mitochondria. Their inadequate positioning results in the observed dampened mitochondrial buffering and elevated intracellular Ca^{2+}. Such changes have the consequence of decreased function of the glutamate transport system, which ultimately triggers the events leading to neuronal death. In this setting, the concentration of extracellular glutamate would be elevated at the synapse, resulting in an excessive influx of Ca^{2+} into neurons via NMDA receptors, as supported by our finding that MK-801 attenuated the effects of insufficient Dlp1. When elevated, neuronal Ca^{2+} yields excessive ROS production and activation of several phospholipases, nucleases, and proteases, culminating in neuronal damage and death (Figure 9, A and B).

Although our results indicate that altered mitochondrial dynamics in astrocytes results in excitotoxic neuronal damage from impaired glutamate regulation, there are several other mechanisms that could contribute to astrocyte dysfunction and neuronal death that should be mentioned. One such mechanism could be related to the observed increase in intracellular Ca^{2+}. In astrocytes, intracellular Ca^{2+} can induce exocytosis of glutamate through a process termed gliotransmission,[39] which is regulated by mitochondrial handling of Ca^{2+}.[40] Elevated intracellular Ca^{2+} could result in increased astrocytic release of glutamate, in addition to impaired uptake, which would further contribute to excitotoxicity (Figure 9, A and B). Our proposed mechanism (Figure 9) focuses on the activation of metabotrobic receptors by glutamate, followed by Ca^{2+} signaling that proceeds through the ER, the predominant pathway through which glutamate signals in astrocytes.[23] Ionotropic receptors, which allow extracellular Ca^{2+} entry directly on stimulation by glutamate, can contribute toward astrocytic Ca^{2+}, but they do not significantly contribute toward

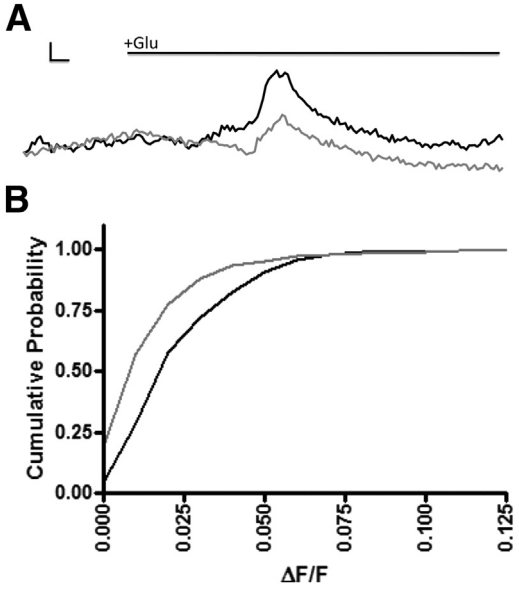

Figure 8 Mitochondrial Ca^{2+} buffering is impaired during glutamate stimulation when astrocyte dynamin-like protein 1 (Dlp1) is knocked down. **A:** Representative images of the mitochondrial Ca^{2+} responses to glutamate in astrocytes transfected with control (ctrl; black line) or Dlp1 (gray line) siRNA. Traces represent mitochondrial Ca^{2+} signals relative to baseline from astrocytes treated with glutamate (black bar). Y scale bar represents 0.01 ΔF/F, and the X scale bar represents 4 seconds. **B:** Cumulative probability plot of the peak amplitude (ΔF/F) of mitochondrial Ca^{2+} responses for astrocytes transfected with ctrl ($N = 7$ replicates/473 cells) and Dlp1 siRNA ($N = 7$ replicates/469 cells). $P < 0.001$ by Kolmogorov-Smirnov test.

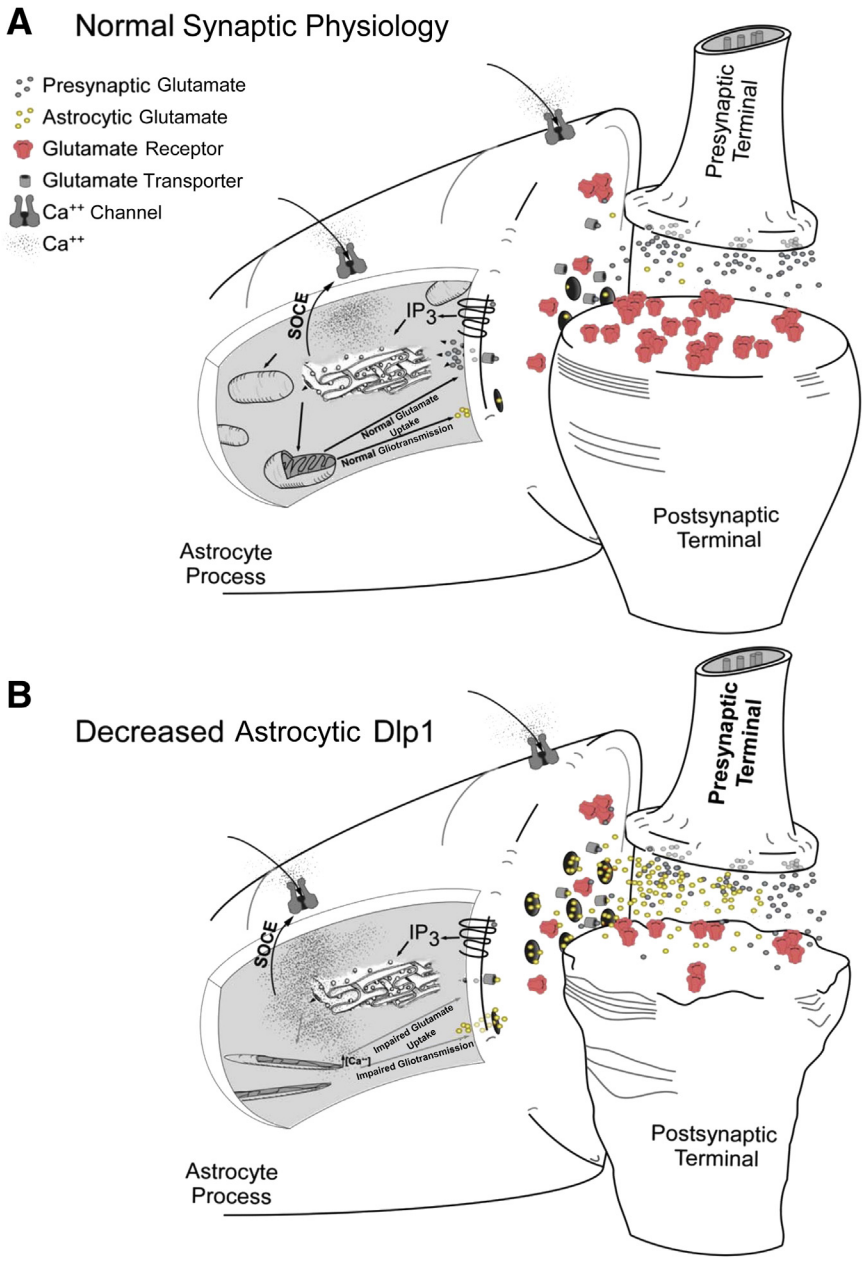

Figure 9 Model of proposed mechanism. **A:** During neuronal glutamate release under normal conditions, glutamate binds to its receptors on astrocytes, and induces release of Ca^{2+} from the endoplasmic reticulum (ER), which causes entry of extracellular Ca^{2+}, primarily via metabotropic receptors, although ionotropic mechanisms may also participate. Mitochondria buffer cytoplasmic Ca^{2+} from each source, astrocytic glutamate uptake occurs, and normal neurotransmission proceeds. **B:** When dynamin-like protein 1 (Dlp1) is decreased in astrocytes, mitochondria are elongated and mislocalized within astrocytic processes. Mitochondria are not adequately positioned to buffer the influx of extracellular Ca^{2+}, resulting in elevated levels of intracellular Ca^{2+} that impair astrocyte-mediated glutamate uptake. Synaptic levels of glutamate are increased as a result, which causes neuronal damage and retraction of the post-synaptic terminal due to excitotoxicity. Astrocytes also release glutamate in a Ca^{2+}-dependent manner in a process called gliotransmission. Elevated intracellular Ca^{2+} that results from decreased Dlp1 could promote excessive glutamate release and contribute to increased synaptic glutamate and excitotoxicity.

astrocytic responses in comparison to ER-mediated Ca^{2+} regulation.[23] Nevertheless, extracellular Ca^{2+} could also enter through the action of ionotropic receptors, and altered mitochondrial regulation of extracellular Ca^{2+} from these sources could also contribute to the observed changes.

Alterations in mitochondrial dynamics resulting from Dlp1 knockdown could also affect other aspects of mitochondrial function that are critical to the cell, including ATP and ROS production, programmed cell death, and mitophagy. Through oxidative phosphorylation, mitochondria produce ATP, with ROS generated as a by-product. The morphological changes that result from decreased Dlp1 could affect not only the amounts of ATP or ROS produced,[41] but also the location within the cell where these products are generated, which could similarly affect glutamate transport.[42–44] Apoptosis is also heavily dependent on mitochondrial dynamics and Dlp1. Apoptotic stimuli promote Dlp1-mediated mitochondrial fragmentation and a release of cytochrome *c*, which results in a caspase cascade and programmed cell death. This process can be prevented by inhibition or knockdown of Dlp1.[45,46] Because this helps to eliminate unhealthy cells, decreased astrocytic Dlp1 could result in lessened removal of impaired astrocytes and reduced neuronal support and protection. The above-described impairment of glutamate transport could also result from decreased mitophagy, a process by which damaged mitochondria are targeted for degradation by autophagy. Dlp1 plays a critical role in this process,[47] and decreasing the expression of Dlp1 would increase the number of

damaged mitochondria in astrocytes or alter the total mitochondrial content of cells, further contributing to the decreased glutamate transport. However, we did not observe changes in total levels of two mitochondrial proteins (MnSOD and cytochrome *c* oxidase; data not shown).

Our study highlights the importance of Dlp1 in astrocytes, an aspect that has not been addressed to date; we also found that Dlp1 was decreased in neurons in PD, which is also a subject worth discussing. Dlp1 is critical in synaptic health, because ablation of Dlp1 impairs proper synaptic pool mobilization and synaptic formation.[48,49] Such findings may have relevance to neurodegenerative diseases because Dlp1 is reported to be decreased in Alzheimer disease brains, similar to our observations in PD. The same study showed decreased dendritic spines and number of spines supported by mitochondria after Dlp1 was knocked down in neurons.[22] This occurred in the face of similar elongated mitochondria, indicating decreased Dlp1 expression in neurons is detrimental toward their health. Moreover, overexpression of Dlp1 in neurons not only increased spine number and synaptic markers, but was protective against neurotoxic protein oligomers.[22] Studies on *Pink1* and *Park2* (coding for the protein Parkin), two genes responsible for familial PD, have tied Dlp1 to PD as well. Knockdown of PINK1 in neurons results in elongated mitochondria, which can be rescued by overexpression of Dlp1.[12] Similar rescue of mitochondrial morphological characteristics, as well as other effects, has been observed when Dlp1 is overexpressed in *Pink1* or *Park2* knockout flies.[13] Dlp1, therefore, serves an important role in neuronal health by promoting adequate mitochondrial positioning within neurons to support proper function, and decreased expression could have detrimental effects. This would mean that the decrease in neuronal Dlp1 in the setting of PD likely represents a process that contributes to neuronal dysfunction and/or death.

In summary, our results show that Dlp1 was decreased in several cell types and multiple brain regions in PD. More important, we demonstrated that astrocyte dysfunction secondary to decreased Dlp1 expression can contribute to neurodegeneration, in part via excitotoxicity. Finally, our data strongly suggest that astrocytic dysfunction due to Dlp1 reduction is coupled to compromised mitochondrial ability to buffer cytosolic Ca^{2+}, which leads to excessive accumulation of extracellular glutamate. Dlp1 also decreases in brain regions without apparent neurodegeneration, which indicates a relatively early event. Correcting this deficiency might be an attractive approach to treat PD patients, especially at early stages.

Acknowledgments

We thank Drs. Michael Robinson, Joshua Jackson, and Jeff Rothstein for helpful and gracious advice and for the antibody for glutamate transporter staining and Drs. Leo Pallanck, Lawrence Loeb, and Thomas Montine for input and guidance that were instrumental in the work presented herein.

J.G.H., T.J.C., T.S., H.M., and J.Z. conceived experiments; J.G.H. and M.T.D. performed tissue studies; J.G.H. and T.J.C. generated cultures and performed transfections; J.G.H. and M.T.D. performed co-culture experiments and measured astrocyte mitochondria; J.G.H. and H.M. performed studies on expression of astrocyte glutamate transporters; J.G.H., T.S., and H.M. contributed to Ca^{2+} imaging experiments and measurements; Z.S.H. generated mechanistic figure; and J.G.H., T.J.C., T.S., Z.S.H., and J.Z. contributed to writing and editing the manuscript.

Supplemental Data

Supplemental material for this article can be found at *http://dx.doi.org/10.1016/j.ajpath.2014.10.022*.

References

1. Schapira AH, Emre M, Jenner P, Poewe W: Levodopa in the treatment of Parkinson's disease. Eur J Neurol 2009, 16:982–989
2. Rinne JO, Portin R, Ruottinen H, Nurmi E, Bergman J, Haaparanta M, Solin O: Cognitive impairment and the brain dopaminergic system in Parkinson disease: [18F]fluorodopa positron emission tomographic study. Arch Neurol 2000, 57:470–475
3. Zgaljardic DJ, Borod JC, Foldi NS, Mattis P: A review of the cognitive and behavioral sequelae of Parkinson's disease: relationship to frontostriatal circuitry. Cogn Behav Neurol 2003, 16:193–210
4. Lees AJ, Hardy J, Revesz T: Parkinson's disease. Lancet 2009, 373: 2055–2066
5. Drukarch B, Schepens E, Stoof JC, Langeveld CH, Van Muiswinkel FL: Astrocyte-enhanced neuronal survival is mediated by scavenging of extracellular reactive oxygen species. Free Radic Biol Med 1998, 25:217–220
6. Rothstein JD, Dykes-Hoberg M, Pardo CA, Bristol LA, Jin L, Kuncl RW, Kanai Y, Hediger MA, Wang Y, Schielke JP, Welty DF: Knockout of glutamate transporters reveals a major role for astroglial transport in excitotoxicity and clearance of glutamate. Neuron 1996, 16:675–686
7. Takada M, Li ZK, Hattori T: Astroglial ablation prevents MPTP-induced nigrostriatal neuronal death. Brain Res 1990, 509:55–61
8. Schapira A, Cooper J, Dexter D, Clark J, Jenner P, Marsden C: Mitochondrial complex I deficiency in Parkinson's disease. J Neurochem 1990, 54:823–827
9. Alam Z, Daniel S, Lees A, Marsden D, Jenner P, Halliwell B: A generalised increase in protein carbonyls in the brain in Parkinson's but not incidental Lewy body disease. J Neurochem 1997, 69:1326–1329
10. Dexter D, Holley A, Flitter W, Slater T, Wells F, Daniel S, Lees A, Jenner P, Marsden C: Increased levels of lipid hydroperoxides in the parkinsonian substantia nigra: an HPLC and ESR study. Mov Disord 1994, 9:92–97
11. Liu W, Acín-Peréz R, Geghman KD, Manfredi G, Lu B, Li C: Pink1 regulates the oxidative phosphorylation machinery via mitochondrial fission. Proc Natl Acad Sci U S A 2011, 108:12920–12924
12. Yu W, Sun Y, Guo S, Lu B: The PINK1/Parkin pathway regulates mitochondrial dynamics and function in mammalian hippocampal and dopaminergic neurons. Hum Mol Genet 2011, 20:3227–3240
13. Poole A, Thomas R, Andrews L, McBride H, Whitworth A, Pallanck L: The PINK1/Parkin pathway regulates mitochondrial morphology. Proc Natl Acad Sci U S A 2008, 105:1638–1643

14. Jin J, Hulette C, Wang Y, Zhang T, Pan C, Wadhwa R, Zhang J: Proteomic identification of a stress protein, mortalin/mthsp70/GRP75: relevance to Parkinson disease. Mol Cell Proteomics 2006, 5: 1193−1204
15. Genda EN, Jackson JG, Sheldon AL, Locke SF, Greco TM, O'Donnell JC, Spruce LA, Xiao R, Guo W, Putt M, Seeholzer S, Ischiropoulos H, Robinson MB: Co-compartmentalization of the astroglial glutamate transporter, GLT-1, with glycolytic enzymes and mitochondria. J Neurosci 2011, 31:18275−18288
16. Danbolt NC, Storm-Mathisen J, Kanner BI: An [Na+ + K+]coupled L-glutamate transporter purified from rat brain is located in glial cell processes. Neuroscience 1992, 51:295−310
17. Storck T, Schulte S, Hofmann K, Stoffel W: Structure, expression, and functional analysis of a Na(+)-dependent glutamate/aspartate transporter from rat brain. Proc Natl Acad Sci U S A 1992, 89: 10955−10959
18. Sattler R, Charlton MP, Hafner M, Tymianski M: Distinct influx pathways, not calcium load, determine neuronal vulnerability to calcium neurotoxicity. J Neurochem 1998, 71:2349−2364
19. Meredith GE, Totterdell S, Beales M, Meshul CK: Impaired glutamate homeostasis and programmed cell death in a chronic MPTP mouse model of Parkinson's disease. Exp Neurol 2009, 219:334−340
20. Vernon AC, Palmer S, Datla KP, Zbarsky V, Croucher MJ, Dexter DT: Neuroprotective effects of metabotropic glutamate receptor ligands in a 6-hydroxydopamine rodent model of Parkinson's disease. Eur J Neurosci 2005, 22:1799−1806
21. Zhang W, Dallas S, Zhang D, Guo JP, Pang H, Wilson B, Miller DS, Chen B, McGeer PL, Hong JS, Zhang J: Microglial PHOX and Mac-1 are essential to the enhanced dopaminergic neurodegeneration elicited by A30P and A53T mutant alpha-synuclein. Glia 2007, 55:1178−1188
22. Wang X, Su B, Lee H, Li X, Perry G, Smith M, Zhu X: Impaired balance of mitochondrial fission and fusion in Alzheimer's disease. J Neurosci 2009, 29:9090−9103
23. Verkhratsky A, Rodríguez JJ, Parpura V: Calcium signalling in astroglia. Mol Cell Endocrinol 2012, 353:45−56
24. Malli R, Frieden M, Osibow K, Zoratti C, Mayer M, Demaurex N, Graier WF: Sustained Ca2+ transfer across mitochondria is essential for mitochondrial Ca2+ buffering, sore-operated Ca2+ entry, and Ca2+ store refilling. J Biol Chem 2003, 278:44769−44779
25. Damier P, Hirsch EC, Zhang P, Agid Y, Javoy-Agid F: Glutathione peroxidase, glial cells and Parkinson's disease. Neuroscience 1993, 52: 1−6
26. Forno LS, DeLanney LE, Irwin I, Di Monte D, Langston JW: Astrocytes and Parkinson's disease. Prog Brain Res 1992, 94:429−436
27. Larsen NJ, Ambrosi G, Mullett SJ, Berman SB, Hinkle DA: DJ-1 knock-down impairs astrocyte mitochondrial function. Neuroscience 2011, 196:251−264
28. Mullett SJ, Hinkle DA: DJ-1 knock-down in astrocytes impairs astrocyte-mediated neuroprotection against rotenone. Neurobiol Dis 2009, 33:28−36
29. Braak H, Sastre M, Del Tredici K: Development of alpha-synuclein immunoreactive astrocytes in the forebrain parallels stages of intraneuronal pathology in sporadic Parkinson's disease. Acta Neuropathol 2007, 114:231−241
30. Bandopadhyay R, Kingsbury AE, Cookson MR, Reid AR, Evans IM, Hope AD, Pittman AM, Lashley T, Canet-Aviles R, Miller DW, McLendon C, Strand C, Leonard AJ, Abou-Sleiman PM, Healy DG, Ariga H, Wood NW, de Silva R, Revesz T, Hardy JA, Lees AJ: The expression of DJ-1 (PARK7) in normal human CNS and idiopathic Parkinson's disease. Brain 2004, 127:420−430
31. Chung EK, Chen LW, Chan YS, Yung KK: Downregulation of glial glutamate transporters after dopamine denervation in the striatum of 6-hydroxydopamine-lesioned rats. J Comp Neurol 2008, 511:421−437
32. Sawada H, Shimohama S, Tamura Y, Kawamura T, Akaike A, Kimura J: Methylphenylpyridium ion (MPP+) enhances glutamate-induced cytotoxicity against dopaminergic neurons in cultured rat mesencephalon. J Neurosci Res 1996, 43:55−62
33. Cornell-Bell AH, Finkbeiner SM, Cooper MS, Smith SJ: Glutamate induces calcium waves in cultured astrocytes: long-range glial signaling. Science 1990, 247:470−473
34. Vermeiren C, Najimi M, Vanhoutte N, Tilleux S, de Hemptinne I, Maloteaux JM, Hermans E: Acute up-regulation of glutamate uptake mediated by mGluR5a in reactive astrocytes. J Neurochem 2005, 94: 405−416
35. Parnis J, Montana V, Delgado-Martinez I, Matyash V, Parpura V, Kettenmann H, Sekler I, Nolte C: Mitochondrial exchanger NCLX plays a major role in the intracellular Ca2+ signaling, gliotransmission, and proliferation of astrocytes. J Neurosci 2013, 33: 7206−7219
36. Boitier E, Rea R, Duchen MR: Mitochondria exert a negative feedback on the propagation of intracellular Ca2+ waves in rat cortical astrocytes. J Cell Biol 1999, 145:795−808
37. Brough D, Schell MJ, Irvine RF: Agonist-induced regulation of mitochondrial and endoplasmic reticulum motility. Biochem J 2005, 392:291−297
38. Kolikova J, Afzalov R, Giniatullina A, Surin A, Giniatullin R, Khiroug L: Calcium-dependent trapping of mitochondria near plasma membrane in stimulated astrocytes. Brain Cell Biol 2006, 35:75−86
39. Mothet JP, Pollegioni L, Ouanounou G, Martineau M, Fossier P, Baux G: Glutamate receptor activation triggers a calcium-dependent and SNARE protein-dependent release of the gliotransmitter D-serine. Proc Natl Acad Sci U S A 2005, 102:5606−5611
40. Reyes RC, Parpura V: Mitochondria modulate Ca2+-dependent glutamate release from rat cortical astrocytes. J Neurosci 2008, 28: 9682−9691
41. Parone PA, Da Cruz S, Tondera D, Mattenberger Y, James DI, Maechler P, Barja F, Martinou JC: Preventing mitochondrial fission impairs mitochondrial function and leads to loss of mitochondrial DNA. PLoS One 2008, 3:e3257
42. Yang Z, Steele DS: Effects of cytosolic ATP on spontaneous and triggered Ca2+-induced Ca2+ release in permeabilised rat ventricular myocytes. J Physiol 2000, 523(Pt 1):29−44
43. Macaskill AF, Rinholm JE, Twelvetrees AE, Arancibia-Carcamo IL, Muir J, Fransson A, Aspenstrom P, Attwell D, Kittler JT: Miro1 is a calcium sensor for glutamate receptor-dependent localization of mitochondria at synapses. Neuron 2009, 61:541−555
44. Wang X, Schwarz TL: The mechanism of Ca2+ -dependent regulation of kinesin-mediated mitochondrial motility. Cell 2009, 136:163−174
45. Gomez-Lazaro M, Bonekamp NA, Galindo MF, Jordán J, Schrader M: 6-Hydroxydopamine (6-OHDA) induces Drp1-dependent mitochondrial fragmentation in SH-SY5Y cells. Free Radic Biol Med 2008, 44: 1960−1969
46. Xie N, Wang C, Lian Y, Zhang H, Wu C, Zhang Q: A selective inhibitor of Drp1, mdivi-1, protects against cell death of hippocampal neurons in pilocarpine-induced seizures in rats. Neurosci Lett 2013, 545:64−68
47. Frank M, Duvezin-Caubet S, Koob S, Occhipinti A, Jagasia R, Petcherski A, Ruonala MO, Priault M, Salin B, Reichert AS: Mitophagy is triggered by mild oxidative stress in a mitochondrial fission dependent manner. Biochim Biophys Acta 2012, 1823: 2297−2310
48. Verstreken P, Ly CV, Venken KJ, Koh TW, Zhou Y, Bellen HJ: Synaptic mitochondria are critical for mobilization of reserve pool vesicles at Drosophila neuromuscular junctions. Neuron 2005, 47: 365−378
49. Ishihara N, Nomura M, Jofuku A, Kato H, Suzuki SO, Masuda K, Otera H, Nakanishi Y, Nonaka I, Goto Y, Taguchi N, Morinaga H, Maeda M, Takayanagi R, Yokota S, Mihara K: Mitochondrial fission factor Drp1 is essential for embryonic development and synapse formation in mice. Nat Cell Biol 2009, 11:958−966